Crystalline structures and crystallization behaviors of poly(L-lactide) in poly(L-lactide)/graphene nanosheet composites

Li, Jingqing; Xiao, Peitao; Li, Hongfei; Zhang, Yao; Xue, Feifei; Luo, Baojing; Huang, Shaoyong; Shang, Yingrui; Wen, Huiying; Christiansen, Jesper De C.; Yu, Donghong; Jiang, Shichun

Published in:
Polymer Chemistry

DOI (link to publication from Publisher):
10.1039/c5py00254k

Publication date:
2015

Document Version
Publisher's PDF, also known as Version of record

Polymer Chemistry

PAPER

View Article Online
View Journal | View Issue

Cite this: *Polym. Chem.*, 2015, **6**, 3988

Crystalline structures and crystallization behaviors of poly(L-lactide) in poly(L-lactide)/graphene nanosheet composites

Jingqing Li,[a] Peitao Xiao,[a] Hongfei Li,*[b] Yao Zhang,[a] Feifei Xue,[a] Baojing Luo,[a] Shaoyong Huang,[c] Yingrui Shang,[a] Huiying Wen,[d] Jesper de Claville Christiansen,[e] Donghong Yu[f] and Shichun Jiang*[a]

Poly(L-lactide) (PLLA)/graphene nanosheet (GNS) composites and pure PLLA were prepared by the solution blending method. Crystalline structures and crystallization behaviors of PLLA in the composite were investigated by XRD, POM, SAXS, and DSC. It was found that α′ form PLLA formation seemed to be more preferred than α form PLLA formation in PLLA/GNS composites at crystallization temperatures T_cs within the α′–α crystal formation transition region due to the existence of GNSs, resulting in an obvious shift of the α′–α crystal formation transition of PLLA in PLLA/GNSs towards high T_cs compared with that of pure PLLA. At T_cs below α′–α crystal formation transition, the formed α′ crystal turned to be more imperfect due to GNS addition, while at T_cs above α′–α crystal formation transition, the crystal structure of α form PLLA was not affected by GNSs. Further POM observations at high T_cs with only α crystal formed showed that PLLA spherulites were well formed in both PLLA/GNSs and pure PLLA, however with very different crystallization kinetics while isothermally crystallizing at different T_cs. The PLLA crystallization process of PLLA in PLLA/GNSs was accelerated by GNSs with both the nucleation rate and spherulite growth rate increased mainly because of the increasing segmental mobility of PLLA chains due to GNS addition; whereas, GNSs showed no observable influence on the determined zero growth temperature T_{zg} of α form PLLA and the T_{zg} was estimated lower than the equilibrium melting point of PLLA, indicating that the crystal growth of PLLA is mediated by a transient mesophase with the transition temperature of T_{zg} between the mesophase and melt not influenced by GNSs in PLLA. Synchrotron on-line SAXS results revealed that the long periods of PLLA in PLLA/GNS composites isothermally crystallized at different T_cs are much smaller than those in pure PLLA. The GNSs are helpful in forming more perfect recrystallized α form PLLA after the α′ form PLLA is melted with increasing T_cs. The presence of GNSs resulted in imperfect α form PLLA from melt directly when it is isothermally crystallized at different T_cs within the temperature range of α′–α crystal formation transition.

Received 15th February 2015,
Accepted 15th April 2015

DOI: 10.1039/c5py00254k

www.rsc.org/polymers

1. Introduction

Poly(L-lactide) (PLLA) is one of the most important environmentally friendly semi-crystalline polymeric materials which can be produced from renewable carbon sources. Many researchers believe that PLLA is a powerful potential alternative for fossil-based polymers. PLLA has already been successfully industrialized and has been found to possess excellent mechanical performance and good biocompatibility, which has made it possible for PLLA to be widely used in different fields.[1–17] For example, it has been successfully used in biodegradable and biocompatible packings and artificial scaffold and drug delivery carriers.[1,2] However, the demands in some special fields are complex and it is difficult for pure PLLA to meet them all. As is known, polyethylene can be melt-blown

[a]*School of Materials Science and Engineering, Tianjin University, Tianjin 300072, P. R. China. E-mail: scjiang@tju.edu.cn*
[b]*State Key Laboratory of Polymer Physics and Chemistry, Changchun Institute of Applied Chemistry, Chinese Academy of Sciences, Changchun 130022, P. R. China. E-mail: hfli@ciac.ac.cn*
[c]*Key Laboratory of Polymer Eco-materials, Changchun Institute of Applied Chemistry, Chinese Academy of Sciences, Changchun 130022, P. R. China*
[d]*College of Engineering and Technology, Northeast Forestry University, Harbin 150040, P. R. China*
[e]*Department of Mechanical and Manufacturing Engineering, Aalborg University, DK-9220, Aalborg, Denmark*
[f]*Department of Biotechnology, Chemistry, and Environmental Engineering, Aalborg University, DK-9000, Aalborg, Denmark*

into agricultural films and finds remarkable applications in agricultural crop production; whereas, low melt strength and low crystallization rate of biodegradable PLLA during the melt-blowing process limit its applications in agriculture compared with polyethylene. Modifications of PLLA would be needed to meet such requirements as well as those in other applications. Since the properties and applications of PLLA or modified PLLA-based materials are closely related to their structural characteristics, the crystal and crystalline structures, crystallization behaviors and crystallization mechanism of the materials have attracted the attention of many researchers[3,12–17] seeking efficient modification methods for PLLA.

In PLLA, three main crystal forms can usually be formed, including α, β, and γ crystal forms. Among them, the α form is orthorhombic and has a 10_3 helical chain conformation and it is the most stable one and can usually be prepared from melt or solution.[8,12] As reported by many researchers,[7,12,15–17] the α form has a disordered form of the α′ form which has been experimentally proved as a new crystalline different from the α form in terms of its disordered helical chain conformation and disordered chain packing mode[5,15,18] and usually can be obtained at a relatively low crystallization temperature T_c from PLLA melt. The β form is an orthorhombic unit cell with a 3_1 helical conformation and can be obtained by stretching at a high drawing rate and high drawing temperature.[3,8] The γ form can be formed at slightly low temperatures when PLLA crystallizes epitaxially on hexamethylbenzene.[17] Here it should be noticed that formation of the α form from melt is dependent on T_c [12] and there is an existence of crystal formation transition from α crystal to α′ crystal with decreasing T_c, which is called "α′–α crystal formation transition" in this work. This means, PLLA can crystallize as the α form when T_c is higher than 120 °C, while the α′ form would appear together with the α form if T_c is controlled between 120 °C and 90 °C. And when T_c is lower than 90 °C, only the α′ form was obtained and the α form was not detectable. If α′ form PLLA is further increased to high temperatures, it can transform into α form PLLA by melting and re-crystallizing,[12] which is called "α′–α crystal transition" in this work. In the past few years, many researchers and groups have focused on the crystal structure variations together with the crystallization behaviors of PLLA after different modifications by tuning the processing conditions,[1,3–5] blending with other materials,[6–8] and adding different kinds of additives to PLLA.[9–11] And the resulting structures and properties of the modified PLLA-based materials were investigated[1,4–11] to further understand the crystallization behaviors and even the crystallization mechanism of PLLA influenced by different factors.

It has been revealed that the lamellar orientation, long periods, and crystal structures of PLLA are dependent on shear conditions, including temperatures, shear rates, and shear strains.[1,5] For example, Huang *et al.*[5] found that melt shear flow favors formation of the α form more than the α′ form, resulting in a shift of α′–α crystal formation transition towards low temperatures, and melt shear can remarkably shorten inducement time and act as a nucleation agent.[5] Wang *et al.*[19] found that the applied melt shear could enhance nucleus density but could not affect the spherulite growth rates of PLLA. This indicated that the crystalline structure and crystallization kinetics of PLLA can be tuned by processing conditions which can obviously affect the states and behaviors of the PLLA molecular chains before and while they enter the crystals.

By blending with other materials,[6–8] the structures and properties of PLLA can also be tuned. Pan[6] reported that crystallization of PLLA could be hindered by the dilution effect of poly(D,L-lactide) (PDLLA) miscible with PLLA at all compositions. This dilution effect of PDLLA is different from the acceleration effect of melt shear reported by Huang *et al.*[5] but formation of α form crystal was also favored and the critical temperatures of α′–α crystal formation transition are reduced from those of pure PLLA. Pan[6] proposed that formation of α′ form crystals of PLLA is kinetically preferential, while that of the thermally stable α form crystals is thermodynamically favored. From this point of view, PDLLA and melt shear mainly affected PLLA crystallization kinetically and thermodynamically, respectively. Lai[8] blended PLLA with 1,3:2,4-dibenzylidene-D-sorbitol (DBS) and found that DBS favored the order and regular α form of PLLA as well as melt shear and dilution effect of PDLLA and at lower temperatures more α form crystal were formed, which made the α′–α crystal formation transition temperature of PLLA shift towards lower temperature as more DBS was added. It was proposed that DBS molecules are stacked together through π–π interaction to form a strand with PLLA molecules by hydrogen bonding and this makes PLLA have a more regular structure but its equilibrium melting point and glass-transition temperature were not significantly changed. Similar to the effect of PDLLA, DBS also decreased the crystallization rate of PLLA though more DBS may act as a nucleation agent, which was attributed to the variation of the crystal structure of PLLA by the authors. This explanation about the decrease of PLLA crystallization rate is different from that reported by Pan[6] in PLLA/PDLLA.

Different kinds of additives are always used as nucleation agents or other functional additives of polymeric materials, especially some typical nano additives developed in recent years.[9–11,20–48] The additives include exfoliated graphite,[9] carbon nanotubes[11,25–34] including single wall carbon nanotubes[29–33] and multi-walled carbon nanotubes,[11,34] graphite oxide,[38–40] graphene nanosheets (GNSs),[10,20–24] montmorillonite,[35–37] layered silicates,[41] and other additives.[42–45] It has been found that many of these additives can be used to tune the mechanical performance of the filled polymeric composites by tuning their crystallization behaviors and crystalline structures, including crystallization kinetics and crystalline morphology.[10,26–32,34–37,41–43] And many of them have been used to modify the properties and structures of PLLA.[9–11] For example, Kim[9] reported that addition of exfoliated graphite to a PLLA matrix to form nanocomposites could enhance the material's thermal stability, mechanical modulus, and electrical conductivity. Villmow[11] dispersed multi-walled carbon

nanotubes in a poly(lactic acid) matrix by tuning twin-screw extrusion conditions and found an electrical percolation threshold was reached below 0.5 wt% MWNT content. With thermally reduced graphene oxide (tr-GO) as the initiator, Yang[49] prepared PLLA/tr-GO composites *via in situ* ring-opening polymerization of lactide and found the thermal stability, crystallization rate, and electrical conductivity of the materials were increased. Wang[39,50] reported that graphene oxide (GO) could accelerate the nonisothermal cold crystallization and isothermal crystallization nucleation density of PLLA, indicating that GO may act as a nucleating agent for PLLA, while the crystallization mechanism and crystal structure remained unchanged at T_c = 130 °C. Chen[40] found that GOs accelerated PLLA crystallization from melt by increasing the nucleation density and addition of 0.1 wt% GO resulted in a small increase of equilibrium melting point but more GOs were unfavorable for the crystallites perfection of PLLA and resulted in a slight decrease of equilibrium melting point.

Xu[10] reported that GNSs could serve as heterogeneous nucleation agents of PLLA as well as CNTs, shortening the induction period of crystallization and accelerating the crystallization kinetics of PLLA, but the induction ability of GNSs was weaker than that of CNTs. In addition, more CNTs in PLLA from 0.05 to 0.1 wt% resulted in a shortened induction period and an enhanced crystallization rate, but the same increasing content of GNSs resulted in a longer induction period and a decreased crystallization rate. The crystallization mechanism of PLLA influenced by GNSs and CNTs was also discussed in detail. Xu[10] explained that in the case of neat PLLA, the conformational ordering during crystallization begins with $-CH_3$ interchain interactions which preceded $-(COCtCH_3)$ interchain interactions. Conversely, in the CNT and GNS nanocomposites, strong noncovalent binding between nanoparticles and PLLA main chains made the conformational ordering begin with $-(COCtCH_3)$ interchain interactions which preceded $-CH_3$ interchain interactions, resulting in a direct reduction of the induction period. This type of interchain interactions could be explained in terms of surface-induced conformational order (SICO). Furthermore, Xu[10] proposed that PLLA chains might prefer to align along the CNT axis and strict lattice matching between PLLA chains and the external graphitic sheet of CNTs is not required; although lattice matching plays a dominant role in surface-induced crystallization of PLLA chains on GNS surface, which makes PLLA chains need more time to adjust their conformations, and PLLA single crystals on GNS surface can show multiple orientations, which might impinge on adjacent single crystals and suppress the crystal growth.

The effect of coexistence of processing conditions and blending with other materials or additives on crystalline structures and crystallization behaviors of PLLA as well as other polymers was also investigated.[23,25,27,29–31,35] Zhang[7] prepared highly oriented and amorphous PLLA/poly(D-lactide) (PDLA) with a 1 : 1 blend of high-molecular-weight PLLA and middle-molecular-weight PDLA. After suitable annealing treatment, the obtained blend crystallized as α′ form crystal together with stereocomplex β_c co-existing in the materials. Such results indicated that a strong enough stretch of PLLA chains favors α′ form crystal formation more than that of the α form, which is different from the results of Huang *et al.*[5] Perhaps, too strong a stretch of PLLA chains inhibited the perfect adjustment of helical chain conformation and the ordered chain packing, resulting in a disordered crystal as the α′ form instead of the ordered α form. In the following heating process above 120 °C, the heavily stretched PLLA chains could relax to some extent and this α′ form crystal could reorganize as the oriented α form which melted around 180 °C. Further heating resulted in crystallization of molten chains on the surface of β_c crystallites with a high degree of chain orientation revealing that β_c crystallite surface has model effects and can induce PLLA molten chains to crystallize on it.

Among the mentioned additives, two-dimensional GNSs have emerged as a subject of enormous scientific interest due to their exceptional electron transport capability, mechanical properties, and high surface area.[2,10,11,20–24] The nucleation effect of GNSs and their influence on crystal structure and crystallization mechanism of PLLA as well as the influences of other modification methods of PLLA have been investigated. However, some details of the influence of GNSs on crystallization behaviors and crystalline structures of PLLA in PLLA/GNS composites have not been fully investigated. For example, the influence of GNSs on the spherulite growth rate and α′–α crystal formation transition of PLLA has been rarely reported. The crystallization mechanism of PLLA and the influences of GNSs on it need further explorations.

To understand the crystallization behaviors and crystallization mechanism of polymers, a crystallization theory of Hoffman–Lauritzen with the popular expression given by eqn (1) has been developed and widely used to describe the temperature dependence of the growth rate u near the melting temperature.[12] Within such a temperature range, the growth rates are considered to be controlled by an activation step. As shown in eqn (1), the first exponential factor accounts for the temperature-dependent segmental mobility as given by the Vogel–Fulcher equation with T_A and T_V referring to the activation temperature and Vogel temperature, respectively.[51,52] The second exponential factor states that the height of the activation barrier diverges at T_f^∞. That is, in the Hoffman–Lauritzen theory, the growth rate of polymer crystallites is usually taken for granted to be controlled by the supercooling below the equilibrium melting point of a macroscopic sample, T_f^∞.

$$u = u_0 \exp\left(\frac{-T_A}{T - T_V}\right) \exp\left(\frac{-T_G}{T_f^\infty - T}\right) \quad (1)$$

Strobl[51] suspected that the activation energy does not diverge at T_f^∞ but much earlier at T_{zg}. He defined T_{zg} as the zero growth temperature which is another characteristic temperature for a system different from T_f^∞. And T_{zg} can be identified with the temperature of the hidden transition between the melt and mesophase according to the Strobl crystallization theory of polymers. Strobl[52] replaced T_f^∞ in eqn (1) with T_{zg}

and eqn (2) was obtained. Then he reordered eqn (2) as eqn (3) with a differentiation of $\ln(u)$ with regard to T. By plotting $[-\mathrm{d}\ln(u/u_0)/\mathrm{d}T + T_A/(T - T_V)^2]^{-1/2} \sim T$, T_{zg} of some polymers can be easily obtained according to the linear relation in eqn (3). For example, T_{zg} of poly(ε-caprolactone) (PCL) had been determined as 77 °C,[51,52] about 22 °C lower than T_f^∞ of PCL. T_{zg}s of iPS and linear PE had been obtained as 275 °C and 132.5 °C, respectively. The existence of T_{zg} of the polymers supported the view of Strobl,[52] showing that the crystal growth is mediated by a transient mesophase with T_{zg} as the transition temperature between it and the melt.

$$u = u_0 \exp\left(\frac{-T_A}{T - T_V}\right)\exp\left(\frac{-T_G}{T_{zg} - T}\right) \quad (2)$$

$$\left(-\frac{\mathrm{d}\ln(u/u_0)}{\mathrm{d}T} + \frac{T_A}{(T - T_V)^2}\right)^{-1/2} = {T_g}^{-1/2}(T_{zg} - T) \quad (3)$$

In this paper, GNSs are added into PLLA by the solution blending method. The crystal structures, crystallization morphology, crystallization behaviors including the nucleation process and spherulite growth of PLLA in the obtained PLLA/GNS composites as well as those of pure PLLA were investigated by XRD, POM, SAXS, and DSC. The influences of GNSs on the crystal forms in PLLA/GNSs and pure PLLA isothermally crystallized at different crystallization temperatures T_cs were first examined to understand the influence of GNSs on the known α′–α crystal formation transition of PLLA. Then T_cs were selected to reveal the nucleation effect of GNSs and the influence of GNSs on the spherulite growth of α form PLLA during the isothermal crystallization process. The resulting crystallization behaviors of PLLA in both PLLA/GNSs and pure PLLA were analyzed according to the Strobl crystallization theory with the zero growth temperature T_{zg}s of α form PLLA in both PLLA/GNSs and pure PLLA determined. With further synchrotron on-line SAXS and DSC results of the variations of long period L of α form PLLA during the isothermal crystallization process and the melting behaviors of both PLLA/GNSs and pure PLLA at different T_cs, and the crystallization mechanisms of PLLA and the influence of GNSs were discussed.

2. Experimental

2.1 Materials

Poly(L-lactide) (PLLA) was supplied by Zhejiang HISUN Biomaterial Co. Ltd, China. The weight average molecular weight (M_w) and the number average molecular weight (M_n) are 109 000 and 88 200 g mol^{-1}, respectively. The differential scanning calorimetry (DSC) determined melting point of the PLLA is 172 °C.

Graphene nanosheets (GNSs) were carboxyl graphene powder productions purchased from Nanjing XFNANO Materials Tech Co., Ltd, which were prepared by thermal exfoliation reduction and hydrogen reduction. The carboxyl content is about 5%. The diameter is about 500 nm. The thickness is about 0.8–1.2 nm. The single layer ratio is 80% and the purity is 99.8%.

2.2 Preparation of PLLA/GNS composites

PLLA was solution blended with GNSs. First, 1 g PLLA was dissolved in 20 mL chloroform. Second, 1 mg GNSs was well dispersed and suspended in DMF by 20 min heating and stirring followed by 20 min ultrasonic treatment. Then the above PLLA solution and GNS suspension were mixed together. With a slow enough addition of alcohol while stirring, PLLA and GNSs were precipitated together. The obtained flocculent precipitate was collected and dried in a vacuum chamber for 24 hours at 70 °C to remove the solvents.

2.3 Sample preparation and characterization

A Linkam CSS450 shear stage (Linkam Scientific Instruments, Ltd, Tadworth, Surrey, UK) was used to prepare samples of pure PLLA and the prepared PLLA/GNS composites at different isothermal crystallization temperatures for XRD, SAXS, and DSC measurement. The mechanical design and electronics of the Linkam shear stage provided a precise control of the needed temperature and sample thickness. An Olympus BX51 was used to obtain POM images. All samples were firstly melted at 200 °C for 1 min on the shear stage, which is connected with a heating and temperature control equipment. Then the upper lid was put on the melted samples, and then most of the bubbles were degassed. Then screwing down the nuts on the upper lid, part of the bubbles were degassed during the process. Then after screwing up the nuts and screwing down the nuts three times, bubbles could be avoided or mostly degassed. After the thermal history of the samples was erased, the samples were cooled with a cooling rate of 30 °C min^{-1} to pre-set temperatures for isothermal crystallization, which were selected as 86 °C, 96 °C, 106 °C, 116 °C, 126 °C, and 136 °C. After being held at the pre-set isothermal crystallization temperatures for enough time to crystallize, the samples were quickly cooled to 30 °C and carefully removed for investigation by *ex situ* XRD and DSC or *in situ* SAXS.

XRD measurements were performed at room temperature using Rigaku D/max 2500 V with a Cu-K_α source (λ = 1.54 Å). The scanning speed is 2° min^{-1} within the range of 10–35°. The voltage is 40 kV and the current is 200 mA.

The synchrotron SAXS measurements were carried out at beamline 1W2A (λ = 1.54 Å) of the Beijing Synchrotron Radiation Facility (BSRF), Beijing, China. 2D-SAXS patterns were integrated to obtain 1D-SAXS profiles as a function of scattering vector. The detector Mar165CCD, with 2048 × 2048 pixels and 79.1 μm pixel size, is 1620 mm away from the sample. The long period of PLLA was calculated according to one-dimension electron density correlation function as shown in ref. 53.

DSC experiments were carried out using Perkin-Elmer DSC-7; the heating rate was 10 °C min^{-1}. The samples of about 10 mg were protected by N_2. The experimental temperature range was selected from room temperature to 200 °C.

3. Results and discussion

3.1. Crystal structures

Since different crystals can be formed in PLLA and the formed crystal structures are dependent on the crystallization temperatures T_cs,[12] the influence of GNSs on the crystal formation of PLLA in PLLA/GNS composites at different T_cs was first examined. Fig. 1(a1) shows the XRD profiles of pure PLLA isothermally crystallized at various T_cs from melt. Fig. 1(a2) and (a3) provide partially enlarged XRD profiles of those in Fig. 1(a1) for pure PLLA. In these XRD profiles of pure PLLA, the most intense peaks can be observed at 2θ = 16.54° for T_cs above 116 °C, which agrees well with the most intense peaks in the WAXS profiles of PLLA located at 2θ = 16.70° for T_cs above 120 °C reported by Kawai *et al.*[12] The peak at 2θ = 16.54° can be attributed to (110) and/or (200) planes. Another strong reflection of (203) and/or (113) planes can also be observed for T_cs above 116 °C. Both these strong peaks remained when T_cs were smaller than 116 °C; whereas several reflections such as (010) and (210) were relatively weak. Since it is known that only α form PLLA can be formed when T_c is higher than 120 °C, the XRD profiles in Fig. 1(a1)–(a3) for T_cs above 116 °C can be assigned to be orthorhombic α form PLLA, in which the PLLA molecules are assumed to have a left-handed 10_3 helical conformation.[12,54]

For T_cs below 116 °C, the intensity of some diffraction peaks, including (103)/(004), (1010), and (010), which are characteristics of α form crystal, decreased with decreasing T_c, and finally disappeared at T_c = 86 °C. At the same time, some diffraction peaks, including (200)/(110) and (203)/(113), shifted

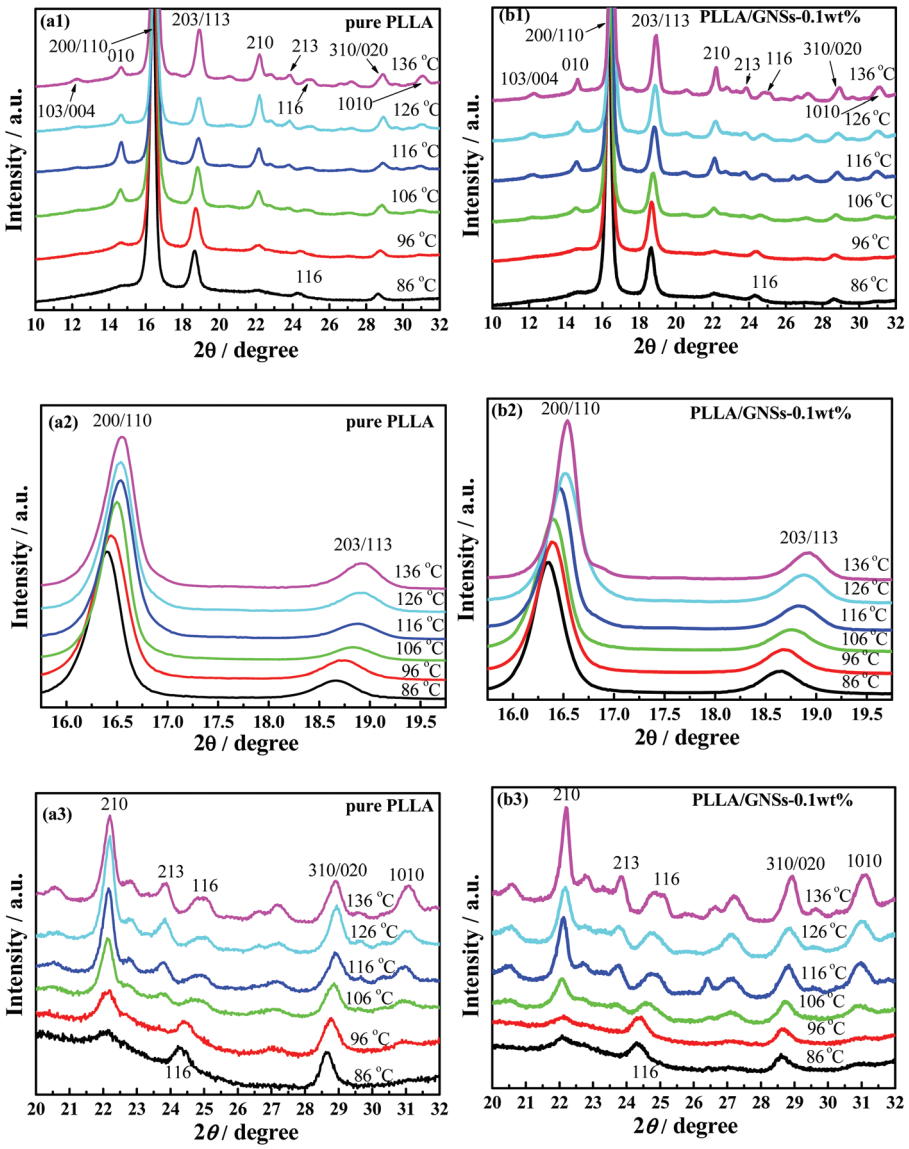

Fig. 1 XRD profiles of pure PLLA and PLLA/GNS composite samples isothermally crystallized at various T_cs from melt (a1)–(a3) pure PLLA, (b1)–(b3) PLLA/GNS-0.1 wt% composites.

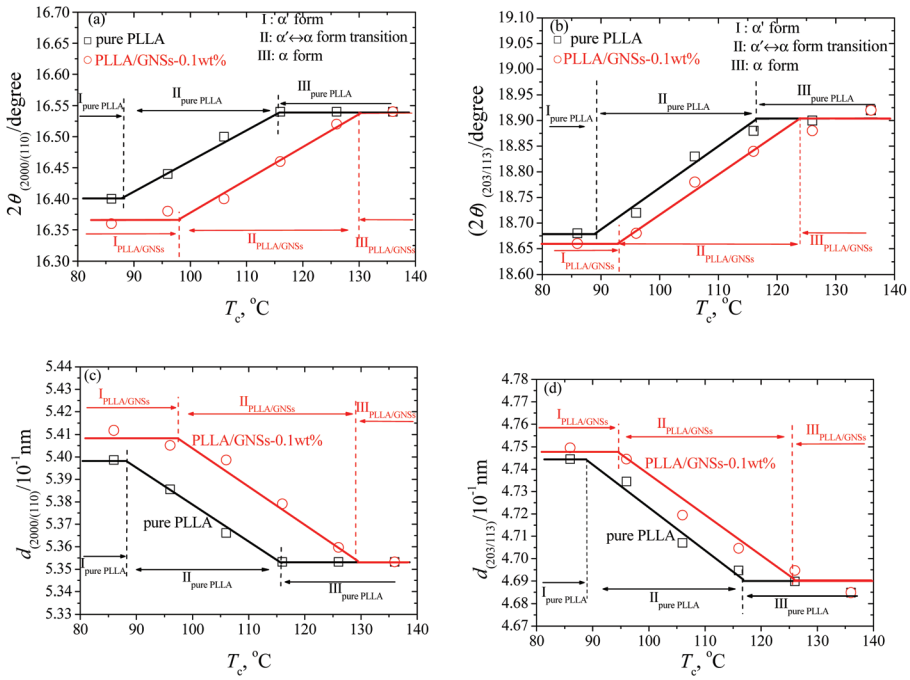

Fig. 2 2θ values from (200)/(110) and (203) diffractions (a and b) and the corresponding d values calculated from the Bragg equation (c and d) of PLLA and PLLA/GNS composite samples crystallized at various T_cs from the melt. The lines are plotted to guide the eyes.

to smaller 2θ values, which were further shown in Fig. 2(a) and (b). These changes of the peaks in XRD profiles of PLLA indicated that the α form content decreased while the α′ form content increased within the isothermally crystallized samples with decreasing T_c till only the α′ form formed below T_c = 86 °C. This agrees with the results of many researchers who regarded the disappearance of the (010) reflection as the indication of crystal formation transitions from co-existence of both α and α′ form to only α′ form PLLA.[3,5,55]

Kawai *et al.*[12] have proved that the disappeared diffraction peaks of (103)/(004), (1010), and (010) in Fig. 1(a1)–(a3) were not due to the crystallinity decrease with decreasing T_c, but due to the crystal structure for lower T_cs which is different from the α form PLLA at higher T_cs. And it seems to be secure to assume this different crystal structure as α′ form PLLA,[1,5–7,12–16] which has a hexagonal packing since the absence of some diffraction can be well explained by the extinction rule of the hexagonal lattice. This was supported by the conclusion drawn from IR measurements by Zhang *et al.*[15,56] which revealed that the PLLA chain has the same 10_3 helical conformation for all T_cs when it is crystallized from the melt and precludes the possibility of β phase formation at low T_cs, proposed by Kawaguchi *et al.*[57]

In Fig. 2(a) and (b), within the experimental range of T_cs, three regions can be observed for the pure PLLA sample: (i) α′ form PLLA below $T_c \approx 86$ °C; (ii) α′–α crystal formation transition with 86 °C < T_c < 116 °C; (iii) α form PLLA above $T_c \approx$ 116 °C. These three regions agree with the results of Kawai *et al.*[12] who concluded by both WAXS and SAXS that the "pure" α′ form might be a limit disordered crystal with hexagonal packing of the 10_3 helix of the PLLA chain and this "pure" α′ form can only be obtained when T_c is below 90 °C. This is somewhat different from the results of Zhang *et al.*[15] who revealed that the α′ form is obtained below 120 °C.

Actually, it is difficult to differentiate the crystal structures of pure PLLA samples only from their XRD profiles shown in Fig. 1(a1), because the crystal structure of α′ form PLLA is quite similar to that of the α form, except for the chain conformation and chain packing mode.[5,58] Since it is known that only α′ crystal and α crystal are formed in the PLLA samples isothermally crystallized at 86 °C and 126 °C, respectively, it is reasonable to regard the (203) reflection peak as one single sharp reflection in XRD profiles of the samples with T_cs of 86 °C and 126 °C. For PLLA samples crystallized at T_cs higher than 86 °C and lower than 126 °C, the (203) reflections can be resolved into two components originating from the co-existing α′ and α form PLLAs. From this point of view, the observed three regions and their relations to crystal forms of PLLA in Fig. 2(a) and (b) within the experimental range of T_cs are acceptable.

Fig. 1(b1) shows the XRD profiles of PLLA/GNS-0.1 wt% composites isothermally crystallized at various T_cs from melt. In Fig. 1(b2) and (b3), these XRD profiles were partially enlarged to show the variations clearly. If one compares the XRD profiles of the composite with those of pure PLLA in Fig. 1(a1)–(a3), one can find that 2θ values of some diffraction peaks, such as (200)/(110), (203)/(113), and so on, of the PLLA/GNS composite samples also shift to smaller values with decreasing T_cs, as shown in Fig. 2(a) and (b). This proved that the α′ form at low T_cs, α′–α crystal formation transition, and α

form at high T_cs of PLLA also appeared in PLLA/GNS composites. Interestingly, it was found that the $2\theta - T_c$ curves of PLLA/GNS composite samples seemed to have moved to higher T_c and smaller 2θ compared with the curves of pure PLLA within the region of α′–α crystal formation transition.

At a high enough T_c, the 2θ values of (200)/(110) and (203)/(113) peaks of XRD profiles of both PLLA/GNS composites and pure PLLA samples tended to be equal. According to the corresponding d values calculated from the Bragg equation of pure PLLA and PLLA/GNS composite samples crystallized from the melt at various T_cs and shown in Fig. 2(c) and (d), the α form PLLA in both the samples has the same crystalline structure at high enough T_cs. This means that the crystalline structure of α form PLLA was not affected by the added GNSs. With decreasing T_c, PLLA/GNS composites enter into the α′–α crystal formation transition region earlier than the pure PLLA sample and their d values are much larger than those of the pure PLLA sample at the same T_c. With T_c decreasing further, PLLA/GNS composites leave the α′–α crystal formation transition region and enter the α′ form region, while the d values of α′ form PLLA in PLLA/GNS composites are obviously much larger than those in the pure PLLA sample. The structure of α′ form PLLA was influenced by GNS addition and tended to be more unstable at T_cs below the α′–α crystal formation transition, which is different from what happened for stable α form PLLA without any variations of d values at high T_cs above the α′–α crystal formation transition.

In addition, in Fig. 2, it is revealed that the added GNSs apparently promoted the crystal formation transition from α form PLLA to α′ form PLLA within the T_c ranges for co-existence of both the crystals; as if α′ form PLLA was preferred more than α form PLLA. That is, GNSs were especially helpful for PLLA to form the less stable α′ crystal instead of the more stable α crystal. If more α′ crystals were formed in a sample, there would be less PLLA molecular chains left to form α crystals. There was a competition between the formation of α′ crystals and α crystals in the samples. This made the primitive α′–α crystal formation transition region in pure PLLA shift to higher temperatures once GNSs were distributed into this material. GNSs made it much easier for α′ crystal to appear even at T_cs higher than 120 °C, under which it was reported that only α crystal can form in pure PLLA. It is indicated that the GNS slices could encourage the PLLA chains to enter the crystal quickly and they seemed to do not have enough time to be well organized to form stable and perfect α crystals, or even form less stable but dense α′ crystals in the PLLA/GNS composites as in pure PLLA.

From Fig. 1 and 2, it can be concluded that a high enough T_c is in favor of a perfect crystalline structure formation of α form PLLA and a low enough T_c makes for only α′ form PLLA in both pure PLLA and PLLA/GNS composite samples. The crystalline structure of α form PLLA at T_cs above the α′–α crystal formation transition was not affected by GNSs, which agreed with Wang *et al.*[50] who reported that both PLLA and PLLA/GOs had the same crystal structure at 130 °C; whereas, the non-perfect α′ form PLLA was influenced and tended to be less perfect at T_cs below the α′–α crystal formation transition. At the same time, GNS existence in PLLA favors α′ crystal formation more than α crystal formation and the α′–α crystal formation transition is shifted to higher temperatures. Such effects of GNSs were different from those of melt shear,[5] PDLLA[6] and DBS[8] all of which favor α crystal formation more inversely and result in shifts of α′–α crystal formation transition towards low temperatures. Melt shear was found to accelerate nucleation of PLLA,[5] while PDLLA and DBS could decrease the crystallization rate of PLLA.[6,8] To understand the influence of GNSs on crystal structures of PLLA further, the crystallization behaviors of PLLA in the composite should be examined and PLLA crystallization mechanism needs to be discussed.

3.2. Crystallization behaviors

In order to know whether the crystallization behavior of PLLA/GNS-0.1 wt% composites is different from that of pure PLLA or not, the POM images of both the materials isothermally crystallized at different T_cs above α′–α crystal formation transition during their isothermal crystallization process were obtained. Thus, the effects of GNSs on the crystallization behavior of α form PLLA were examined.

Fig. 3 shows the typical POM images of the samples at T_c = 140 °C. From Fig. 3, it can be seen that PLLA spherulites were well formed both in pure PLLA and PLLA/GNS-0.1 wt% composite samples during their isothermal crystallization process. This implied that PLLA spherulite formation was not disturbed by GNSs in PLLA/GNS-0.1 wt% composites. While comparing the POM images in Fig. 3(a1)–(a3) with those in Fig. 3(b1)–(b3), one can observe that more PLLA spherulites are formed in PLLA/GNS-0.1 wt% composites than in pure PLLA in the same isothermal crystallization time with T_c = 140 °C within the first 20 min of the crystallization process. This revealed that the nucleation density of α form PLLA in PLLA/GNS-0.1 wt% composites is much higher than that of the pure PLLA sample. That is, the addition of GNSs into PLLA accelerated the nucleation process of PLLA.

From Fig. 3(a4) and (b4), it can be noticed that 100 min and 34 min were needed for PLLA spherulites in pure PLLA and PLLA/GNS-0.1 wt% composite samples, respectively, to grow to full observed range of the POM images. The obtained PLLA spherulites in pure PLLA seemed to be slightly larger than those in PLLA/GNS-0.1 wt% composite samples, which confirmed the higher nucleation density of PLLA in the composite as revealed in Fig. 3(a1)–(a3) and (b1)–(b3). This proved that GNSs could serve as nucleating agents for accelerating the crystallization kinetics of PLLA, agreeing with Xu.[10]

In fact, the increased nucleation density of PLLA spherulites in PLLA/GNS-0.1 wt% contributed to the higher crystallization rate of PLLA in the composites than in pure PLLA. The increased PLLA spherulite growth rate due to addition of GNSs also played important roles. To understand this, the diameters of PLLA spherulites depending on isothermal crystallization time during the crystallization process were obtained and are shown in Fig. 4 for both pure PLLA and PLLA/GNS-0.1 wt%

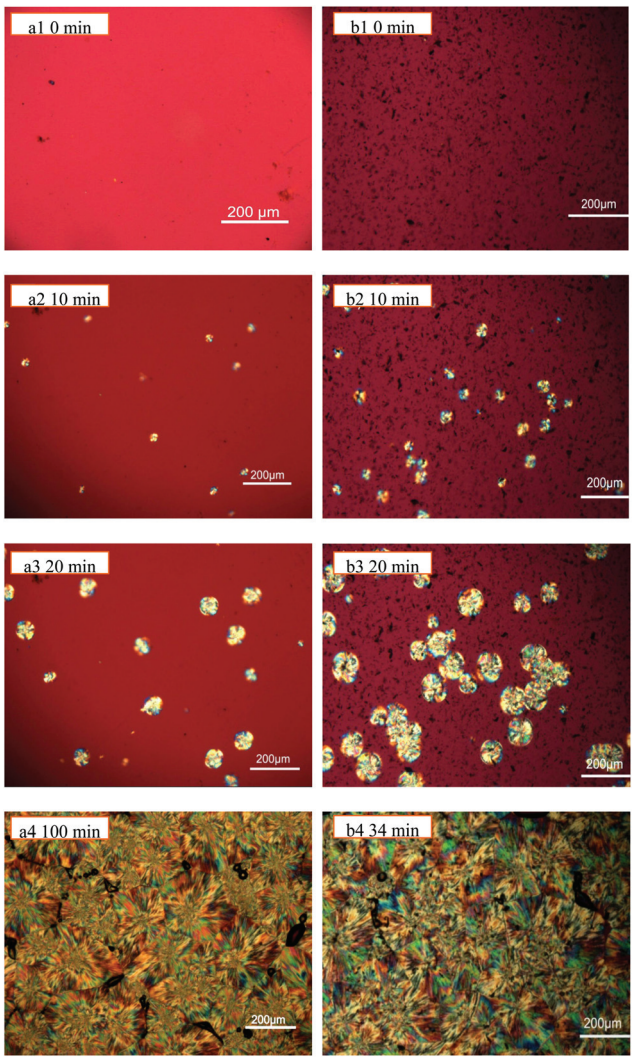

Fig. 3 POM images of PLLA and PLLA/graphene composite samples isothermally crystallized at T_c = 140 °C from melt during their isothermal crystallization process: (a1)–(a4) pure PLLA, (b1)–(b4) PLLA/GNS-0.1 wt% composite.

composite samples. From the slopes of the fitted lines in Fig. 4, the radius growth rates of the PLLA spherulites were determined and are shown in Fig. 5.

According to the crystallization theory, the crystal growth rate always shows well-known bell-shaped temperature dependence. This is also found to be true for pure PLLA and PLLA/GNS-0.1 wt% composite samples. It can be found in Fig. 5 that the radius growth rate of PLLA spherulite of pure PLLA reached its peak value at about T_c = 130 °C. This experimental result agrees very well with that reported by Kawai and his co-workers.[12] Importantly, at all the experimental crystallization temperatures, the radius growth rates of PLLA spherulite of PLLA/GNS-0.1 wt% composite samples were found to be larger than those of pure PLLA samples. GNSs can accelerate the radius growth of PLLA spherulite, but they do not change the well-known bell-shaped temperature dependence of the radius growth rate. GNSs in PLLA/GNS-0.1 wt% composites even had no influence on the position of the peak growth rate at about T_c = 130 °C. From this point of view, the faster crystallization process of PLLA in PLLA/GNS-0.1 wt% composites than that of pure PLLA can be attributed to the combination of the faster nucleation process and the faster radius growth of the spherulite of PLLA in PLLA/GNS-0.1 wt% composites than in pure PLLA.

The DSC curves of pure PLLA and PLLA/GNS-0.1 wt% composite samples during the non-isothermal crystallization process with a temperature decreasing rate of 10 °C min^{-1} from melts shown in Fig. 6 supported the above POM observations. With temperatures decreasing, the DSC curve of the pure PLLA sample showed one exothermic peak. Similarly, PLLA/GNS-0.1 wt% composites also showed one exothermic peak. However, their thermal enthalpy is much larger and the corresponding temperature of the crystallization peak is higher than that of the pure PLLA sample. The thermal enthalpy difference of the two samples implied that GNSs in PLLA/GNS-0.1 wt% composites resulted in higher crystallinity of their PLLA matrix. In the pure PLLA sample, with temperatures decreasing, low nucleation rate and slow radius growth rate of the spherulite apparently did not leave enough time for

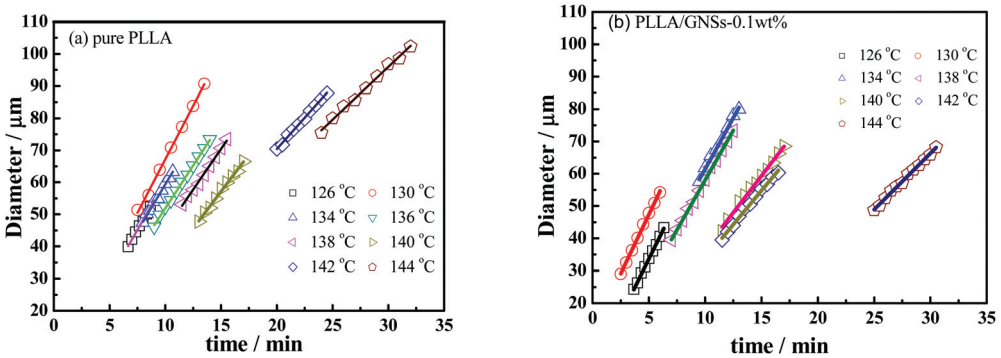

Fig. 4 Diameter growth of spherulites of PLLA and PLLA/GNS composite samples isothermally crystallized at various T_cs from melts: (a) pure PLLA, (b) PLLA/GNS-0.1 wt%.

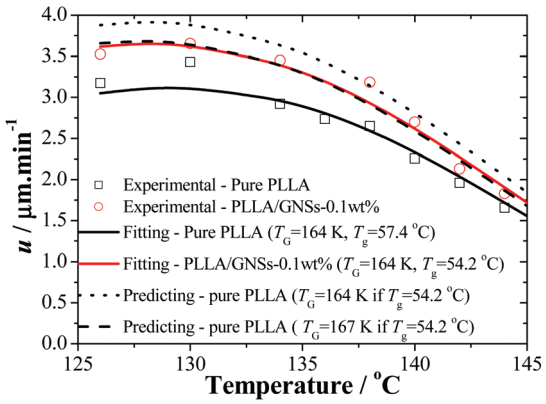

Fig. 5 Radius growth rates u of the spherulites of PLLA in pure PLLA and PLLA/GNS composite samples as functions of crystallization temperature (T_c). Solid lines are obtained by fitting the experimental data according to eqn (3) with T_{zg} = 177 °C and T_g = 164 K. The dotted and dashed lines are the predicting results of pure PLLA according to eqn (3) with T_{zg} = 177 °C and T_g of 164 K and 167 K, respectively, if T_g is set equal to that of PLLA/GNSs of 54.2 °C.

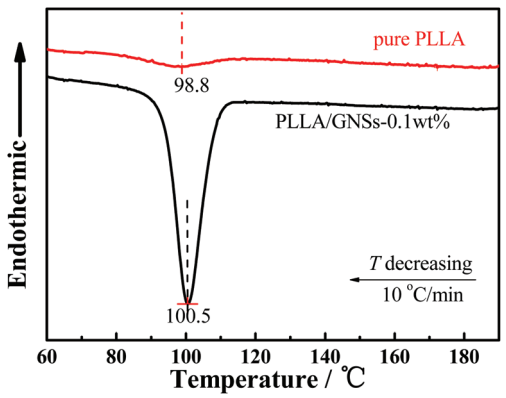

Fig. 6 DSC curves of the non-isothermal crystallization process of PLLA in pure PLLA and PLLA/GNSs composite samples with a temperature decreasing rate of 10 °C min^{-1} from melts.

the concerned PLLA molecular chains to form crystalline structures. When GNSs are added, both the nucleation rate and the radius growth rate of the spherulite are increased. Thus, the total crystallization rate of PLLA is enhanced by GNSs comprehensively in the composite.

It seemed that the added GNSs can provide more chances for more PLLA molecular chains to form crystalline structures within the limited time range before they are cooled to lose enough mobility due to decreasing temperature. It is really an interesting observation. Since GNSs in the composite may act as "physical walls" interacting with the PLLA molecular chains, theoretically the number of chain configurations should decrease and hence there would be less mobility of the PLLA chains which would leave less chances for crystallites to form. However, the opposite was observed here. Maybe the sum of attraction forces along a chain is lower in the presence of a physical wall like a GNS. This leads to less configurational possibilities of PLLA chains – however also to a much higher mobility hence favoring crystallinity.

To find out the effects of GNS addition on the mobility of PLLA molecular chains in PLLA/GNS composites, further DSC measurements were executed to determine the glass transition temperatures of PLLA in pure PLLA and in the composite. The isothermally crystallized samples at different crystallization temperatures T_c were adopted and the onset temperatures of the glass transitions were obtained. The T_cs were selected as 86, 96, 106 and 116 °C and the results are shown in Fig. 7 as examples. The glass transition temperature $T_{g,onset}$ of PLLA in pure PLLA was determined as about 57.4 °C and it was found almost independent on T_c. Importantly, the $T_{g,onset}$ of PLLA in PLLA/GNS composites was about 54.2 °C, also independent of T_c, and it was really found to be lower than the $T_{g,onset}$ of pure PLLA. This meant that the added GNSs in the composite increased the mobility of PLLA molecular chains.

As is known, in PLLA main chains, there are many structures of –(COCtCH$_3$) resulting in strong interchain interactions by hydrogen bonds, while on the surface of GNS slices there are no such polar functional groups. This decrease of the $T_{g,onset}$ of PLLA due to the existence of GNSs in PLLA may be possible. Perhaps the interactions between PLLA chains were weakened since the interactions between GNSs and PLLA chains may be much weaker. The dispersed GNSs in PLLA resulted in replacement of relatively strong interactions between PLLA chains by somewhat weaker GNS–PLLA chain interactions. This could be supported by Patti's[59] studies who proved by molecular dynamics simulations that small nanoparticles can act as plasticizers in a polymeric matrix. Xiao *et al.*[60] reported that the plasticized poly(lactic acid) with triphenyl phosphate (TPP) could increase the spherulite growth rate. Of course, for PLLA chains with too low a mobility to form a crystallization nucleus, increased chain mobility would help PLLA chains to enhance the nucleation density. This well explains why GNSs can accelerate the crystallization process of PLLA.

The kinetic data in Fig. 5 can be reorganized and linearly fitted by plotting $[-\mathrm{d}\ln(u/u_0)/\mathrm{d}T + T_A^*/(T - T_V)^2]^{-1/2} \sim T$ according to eqn (3) and the results are shown in Fig. 8. Here, T_A = 754 K was obtained from $T_A = U^*/R$ with U^* = 1500 cal mol^{-1} and $T_V = T_g - 30$ K was selected according to ref. 12. With the linear fitting parameters of T_{zg} = 177 °C and T_G = 164 K for both pure PLLA and PLLA/GNSs in Fig. 8, the fitted curves of growth rate u dependent on T_c were calculated and are shown in Fig. 5 to compare with those in experimental data. The results showed that both the growth rates of pure PLLA and PLLA/GNSs could be fitted well. Thus, the zero growth temperature T_{zg} of PLLA was determined as 177 °C and it was found that there was no observable influence of the added GNSs on it.

As for pure PLLA, the T_{zg} = 177 °C of α crystal is found to be smaller than T_f^∞ = 192.8 °C reported by Xiao[60] for their PLA 4032D with a melting point of 168 °C. Tsuji[61] reported an even higher T_f^∞ for their samples, in the range from 198 to 212 °C

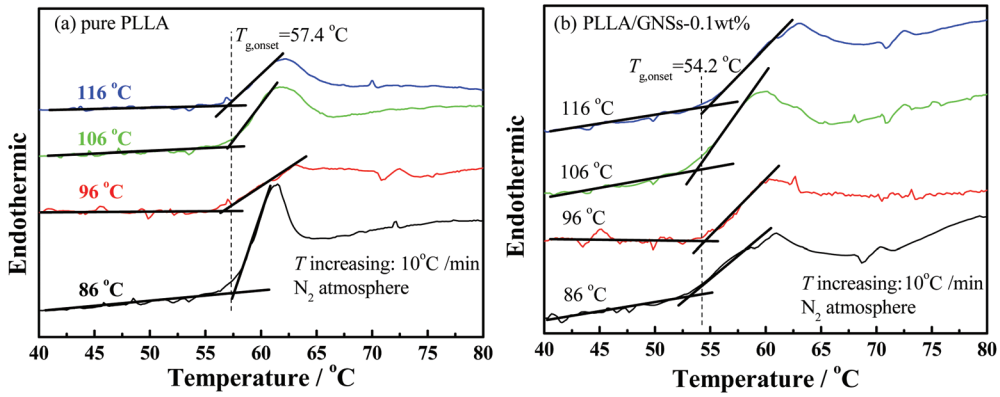

Fig. 7 Determination of glass transition temperatures of PLLA by DSC with a temperature increasing rate of 10 °C min^{-1} for the samples isothermally crystallized at different T_cs: (a) pure PLLA, (b) PLLA/GNSs-0.1 wt%.

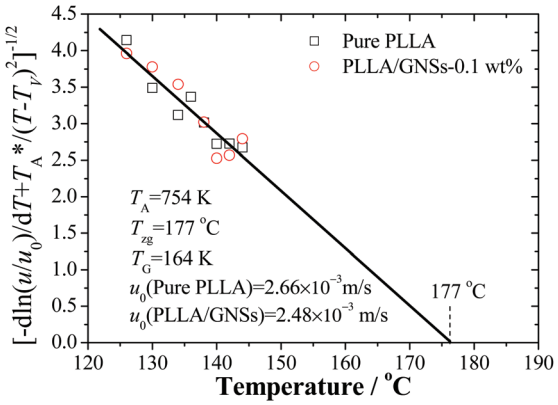

Fig. 8 Analysis of PLLA spherulite growth rate data of pure PLLA and PLLA/GNSs-0.1 wt% composites by fitting with eqn (3) according to the Strobl crystallization theory.

and Kawai *et al.*[12] gave T_f^∞ = 215 °C. Since the used PLLA here has a melting point of 172 °C which is higher than 168 °C, the T_f^∞ may be higher than 192.8 °C. This implies that pure PLLA may have a T_{zg} lower than its T_f^∞. Importantly, the T_{zg} and T_G values of α form PLLA in PLLA/GNSs are found to be equal to those of α crystal in pure PLLA, only with the u_0 values slightly different.

According to eqn (2), lower T_g of PLLA favors a larger growth rate u. But according to eqn (3), at temperatures near T_{zg}, growth rate u tends to be very small and the T_g variation of PLLA has little influence on T_{zg} of α form PLLA. This indicated that the GNS-induced increase of PLLA segmental mobility does not affect the T_{zg} value and only results in decrease of T_G, which has been supported by the fitting results according to eqn (3) in Fig. 8. With increasing T_c, the decrease of spherulite growth rate of PLLA in PLLA/GNSs was accompanied by a synchronous reduction of the acceleration effects of GNSs on the growth rate. It seemed that GNSs had no impact on the thermodynamic essence of the investigated isothermal crystallization process of PLLA, though it can help PLLA spherulites kinetically grow faster, or the influence of GNSs on the isothermal crystallization thermodynamics is too weak to be observed. This may be helpful to understand the effects of GNSs on the crystallization process and the crystallization mechanism of PLLA.

Supposing that T_g of pure PLLA decreased from 57.4 °C to 54.2 °C which is equal to that of PLLA in PLLA/GNSs, a predicting line shown as the dotted line in Fig. 5 could be obtained if the fitting parameters T_{zg} = 177 °C, T_G = 164 K, and u_0 = 2.66 × 10^{-3} m s^{-1} obtained in Fig. 8 were used. It can be seen that the values of the growth rate u at different T_cs are obviously larger than the experimental data and the fitting line of PLLA/GNSs according to the Strobl crystallization theory. When the value of T_G was adjusted to 167 K, the predicting dashed line for pure PLLA in Fig. 5 could overlap well with the fitting line of PLLA/GNSs. This implied that the increase of growth rate u of PLLA in PLLA/GNSs, when compared with that of PLLA in pure PLLA, is mainly due to the increase of segmental mobility of PLLA chains because of addition of GNSs. At the same time, the contribution of the increased segmental mobility seemed to have been inhibited by GNSs which have certain steric hindrance to spherulite growth. This agrees with the results of Xu[10] who found that 0.05 wt% content of GNSs in PLLA could serve as heterogeneous nucleation agents of PLLA, shortening the induction period of crystallization and accelerating the crystallization kinetics of PLLA. However, if GNS content increased to 0.1 wt%, it resulted in a longer induction period and a decreased crystallization rate of PLLA, because PLLA single crystals on GNS surface may suppress the crystal growth.

3.3. Lamellar parameter

To further understand the influence of GNSs on the crystalline structure of PLLA, pure PLLA and PLLA/GNS composite samples were both isothermally crystallized at 145 °C to form α form PLLA and their 2D SAXS patterns were collected. Some typical patterns were selected and are shown in Fig. 9. Corresponding to the 2D SAXS patterns, 1D SAXS intensity profiles were plotted and are shown in Fig. 10.

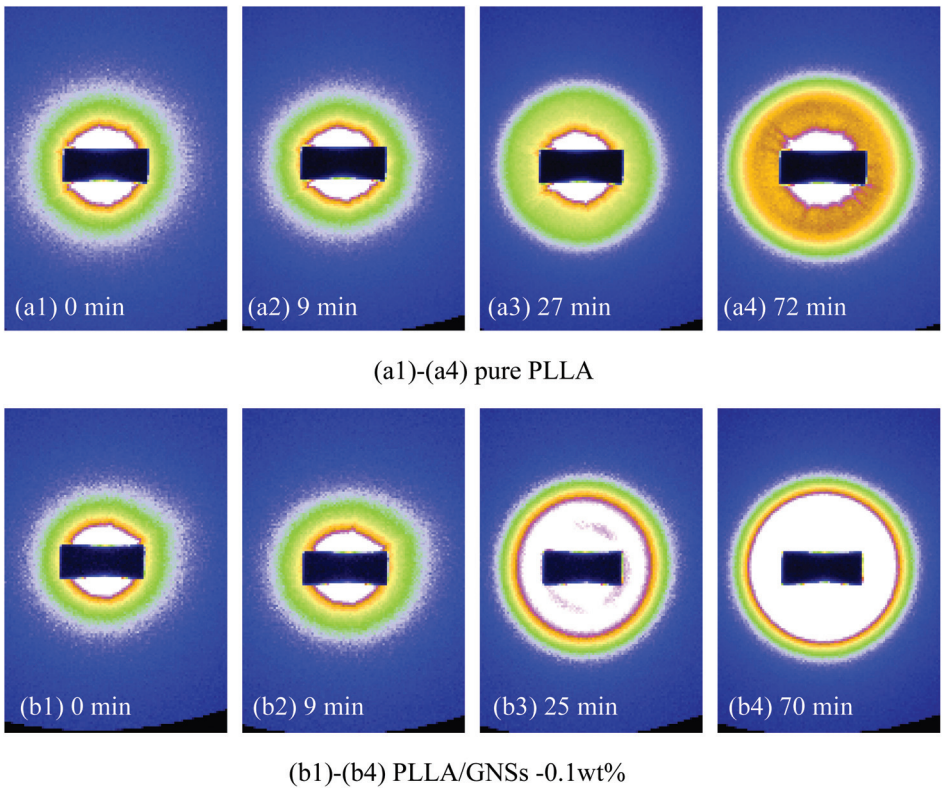

Fig. 9 2D SAXS patterns of pure PLLA and PLLA/GNSs composite samples isothermally crystallized at 145 °C: (a1)–(a4) pure PLLA, (b1)–(b4) PLLA/GNSs-0.1 wt%.

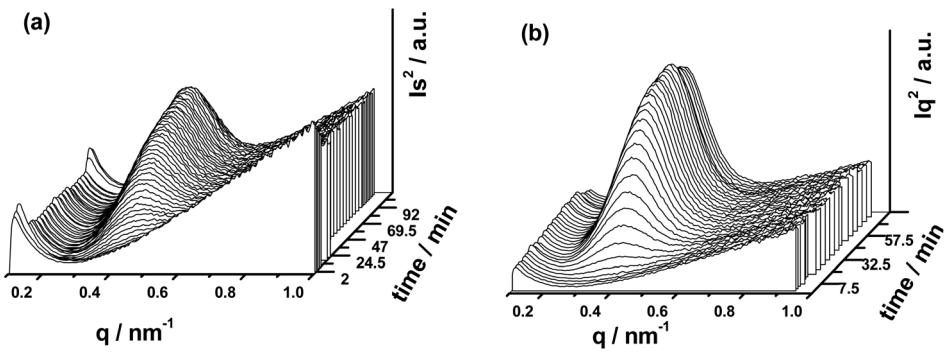

Fig. 10 1D SAXS intensity profiles of pure PLLA and PLLA/GNSs composite samples isothermally crystallized at 145 °C: (a) pure PLLA, (b) PLLA/GNSs-0.1 wt%.

From Fig. 9(a1) and (b1), no observable scattering circles related to crystalline structures of PLLA can be found, indicating that all the crystalline structures in the two samples had already been removed when melted. In Fig. 10(a) and (b), no crystalline peaks appeared in both the samples. With the crystallization time increasing, one scattering circle appeared in the 2D SAXS patterns in Fig. 9 and crystalline peaks appeared in the 1D SAXS intensity profiles in Fig. 10. Then the intensity of the scattering circles of both the samples increased with increasing crystallization time till the samples crystallized completely. From the variations of the intensity of the crystalline peaks in Fig. 10, the inducing crystallization time of pure PLLA and PLLA/GNS composite samples was determined as 14 min and 7 min, respectively. The two samples finished their crystallization processes at about 63 min and 45 min, respectively. This agrees with POM observations.

Fig. 11 shows the long periods of PLLA in pure PLLA and PLLA/GNS composite samples isothermally crystallized at 145 °C dependent on crystallization time. During the crystallization processes, long periods, L, of the two samples decreased

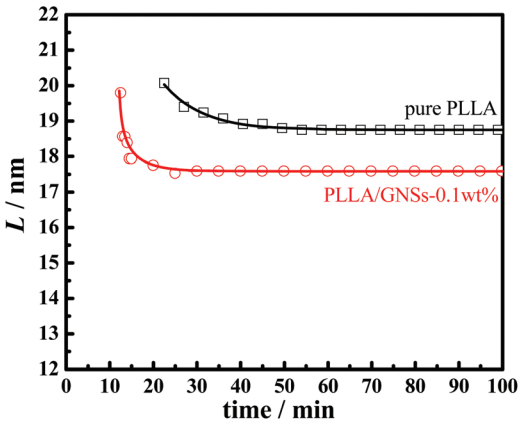

Fig. 11 Lamellar parameter L of PLLA in pure PLLA and PLLA/GNSs composite samples isothermally crystallized at 145 °C as a function of crystallization time.

with increasing isothermal crystallization time and finally reached constant values when crystallization processes finished. Those L values of PLLA/GNS composites were found to be much smaller than those of pure PLLA and the revealed crystallization process finished much earlier than that of pure PLLA.

These phenomena can be interpreted successfully by the Dual-lamellar stack model.[62] At the initial stage of the isothermal crystallization process, some thick lamellar structures were formed first, and then some lamellar structures formed later were inserted into the ones first formed, which resulted in decreasing the long period, L, during the isothermal crystallization process until the process finished. This phenomenon has also been found in other crystalline polymeric systems.[23,27]

3.4. Melting behaviors

As is known, melting behaviors are closely related to the crystallization behaviors and the resulting crystalline structures of crystalline or semi-crystalline polymers. Fig. 12 shows the melting behaviors of pure PLLA and PLLA/GNS composite samples isothermally crystallized at various T_cs from melts revealed by DSC curves. According to the XRD profiles, only α form PLLA were formed at T_c = 136 °C and only α′ form PLLA were formed at T_c = 86 °C in the pure PLLA sample. At T_c = 106 °C and T_c = 96 °C, within the α′–α crystal formation transition region, both α and α′ form PLLAs were formed in the pure PLLA sample. Because α form PLLA is more perfect than α′ form PLLA, the melting point of α form PLLA is higher than that of α′ form PLLA. The pure PLLA isothermally crystallized at T_c = 136 °C showed a melting point of T_m = 173.0 °C, which is higher than T = 170.5 °C of the pure PLLA isothermally crystallized at T_c = 86 °C. T_m = 173.0 °C can be attributed to the melting behavior of α form PLLA formed at T_c = 136 °C, while T = 170.5 °C cannot be directly attributed to the melting behavior of α′ form PLLA formed at T_c = 86 °C. In fact, from the DSC curve of pure PLLA isothermally crystallized at T_c = 86 °C, an exothermic peak at 152.2 °C can be found lower than the obvious endothermic melting peak at T = 170.5 °C. This exothermic peak can be attributed to α′–α crystal transition on increasing the temperatures.[12] So T = 170.5 °C should be attributed to the melting behavior of those reformed α form PLLA in the pure PLLA sample isothermally crystallized at T_c = 86 °C. Interestingly, it seemed that all those α′ form PLLA, formed at T_c = 86 °C, melted and recrystallized as α form PLLA with increasing temperature from a temperature lower than 86 °C to a temperature higher than 180 °C, which makes it difficult to find the endothermic peak related to the melting behavior of α′ form PLLA isothermally crystallized at T_c = 86 °C. Perhaps, the appearance of the exothermic peak at 152.2 °C revealed that the endothermic therapy of α′ form PLLA was less than the exothermic therapy of α′–α crystal transition of PLLA in this pure PLLA sample isothermally crystallized at T_c = 86 °C.

In the DSC curve of pure PLLA isothermally crystallized at T_c = 96 °C, an exothermic peak at 156.2 °C appeared, which is higher than that exothermic peak at 152.2 °C of the sample isothermally crystallized at T_c = 86 °C. The endothermic peak of the melting behavior of the reformed α form PLLA transited

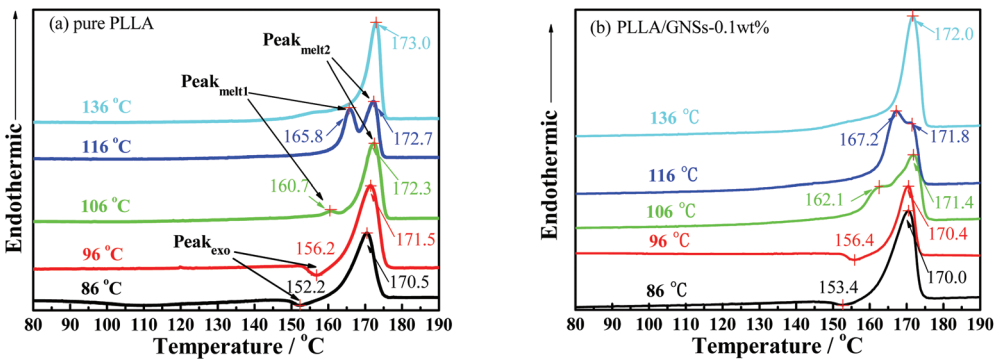

Fig. 12 DSC heating thermographs of pure PLLA and PLLA/GNSs composite samples isothermally crystallized at various T_cs from the melt: (a) pure PLLA, (b) PLLA/GNSs-0.1 wt%.

from α′ form PLLA increased from T_m = 170.5 °C of the sample isothermally crystallized at T_c = 86 °C to T_m = 171.5 °C of the sample isothermally crystallized at T_c = 96 °C. This implied that the α′ form PLLA in the sample isothermally crystallized at T_c = 96 °C is more perfect than that in the sample isothermally crystallized at T_c = 86 °C. The more perfect α′ form PLLA needs higher temperature to melt and transit into the more perfect α form PLLA. With T_c increasing higher than T_c = 96 °C within the α′–α crystal formation transition region, less α′ form PLLA in the sample results in smaller exothermic peaks while melting, which may be smaller than the endothermic melting peaks of these α′ form PLLAs. For example, as shown in Fig. 12(a), the DSC curve of the sample isothermally crystallized at T_c = 106 °C showed a small endothermic peak at T = 160.7 °C, which resulted from a competition between α′–α crystal transition and the melting process of α′ form PLLA.

When GNSs are added into PLLA, the melting behaviors of the composite samples isothermally crystallized at different T_cs, as shown in Fig. 12(b), are almost similar to those of the pure PLLA samples. The T_ms of the α form PLLA in PLLA/GNS-0.1 wt% samples formed during the isothermal crystallization process or reformed from the α′–α crystal transition process are lower than those of the α form PLLA in the pure PLLA sample at T_c = 96 °C, 106 °C and 136 °C, respectively. This indicated that addition of GNSs into PLLA does not change the crystalline forms but prevents the molecular chains of PLLA from forming perfect crystalline structures, because GNSs accelerate the crystallization process and do not leave enough time for PLLA chains to adapt as completely as possible to the strict geometric space of perfect crystals.

In addition, it can be found in Fig. 12(a) and (b) that the α′–α form transformation temperature and T_ms of α′ form PLLA in PLLA/GNS-0.1 wt% samples are higher than those of the pure PLLA sample. The addition of GNSs into PLLA improved the perfectness of α′ form PLLA. The influence of GNSs on the formation of α′ form PLLA is different from that of α form PLLA.

3.5. Crystallization mechanism

As revealed in Fig. 5, the addition of GNSs does not change the temperature corresponding to the fastest radius growth rates u of the spherulites of PLLA. At about T_c > 130 °C, the mobility of PLLA molecular chains in both the pure PLLA and PLLA/GNS-0.1 wt% samples are high enough to form a crystal. This meets with the thermodynamic conditions of formation of α form PLLA, whose formation is controlled by the thermodynamic process.[4,6,8] The addition of GNSs into PLLA seems to have no influence on the thermodynamics of formation of α form PLLA. The larger radius growth rates u of the PLLA spherulites in PLLA/GNS-0.1 wt% than those in pure PLLA can mainly be attributed to the increase of the segmental mobility of PLLA chains due to addition of GNSs. The existing GNSs help PLLA molecular chains enter crystals faster. This is supported by the same zero growth temperature T_{zg} of PLLA in PLLA/GNSs as that of pure PLLA.

Perhaps, during the crystallization process of PLLA, the segmental mobility of the PLLA molecular chains in PLLA/GNS-0.1 wt% is too fast to adapt perfectly into the crystals or the steric hindrance of GNSs to spherulite growth makes it difficult to form perfect crystals. Thus, the α form PLLA formed in PLLA/GNS-0.1 wt% samples is less perfect than that in the pure PLLA sample, resulting in lower T_m of α form PLLA in PLLA/GNS-0.1 wt% samples than in the pure PLLA sample which were isothermally crystallized at T_c = 136 °C. This was supported by the smaller long period L of α form PLLA in PLLA/GNSs than that in pure PLLA at 145 °C. Even in the α′–α crystal formation transition range, T_ms of α form PLLA in PLLA/GNS-0.1 wt% are lower than those in pure PLLA and both of the T_ms of α form PLLA in the two samples decreased with decreasing T_c. It seemed that the effect of GNSs is not obviously conflicted with the low molecular mobility at low temperatures. Perhaps, only those PLLA chains with strong enough mobility but without the steric hindrance of GNSs to spherulite growth can form a perfect α form crystal.

Within the α′–α crystal formation transition range, introduction of GNSs resulted in α′ form PLLA with more perfect crystal structures in PLLA/GNS-0.1 wt% than in pure PLLA at the same T_c. In this temperature range, the mobility of PLLA molecular chains in the pure PLLA sample is too low, resulting in less perfect crystals and low crystallization speed. The existence of GNSs can enhance the mobility of PLLA chains and help them enter the α′ form crystal in a more perfect way. So at the same time, GNSs can improve the perfectness of the formed crystals. These effects of GNSs on α′ form PLLA formation are different from the effects on α form PLLA formation. The formation of α′ form PLLA has been reported to be controlled by its kinetic mechanism[4,6,8] instead of its thermodynamic mechanism. The different effects of GNSs on α and α′ form PLLA should be attributed to their different formation mechanism. With decreasing T_c in the α′–α crystal formation transition range, T_ms of α′ form PLLA in both PLLA/GNS-0.1 wt% and pure PLLA decreased. The effect of GNSs on α′ form PLLA acts together with T_c on the crystallization process, but it does not change the essence of the T_c effect on crystal formation. This implied that the effect of GNSs does not influence the essence of PLLA molecular chain mobility.

The shift of α′–α crystal formation transition of PLLA/GNS-0.1 wt% samples to higher temperatures compared to that of the pure PLLA sample can be interpreted. The acceleration effect of GNSs on the formation of α′ form PLLA is more efficient than the formation of α form PLLA. At the same T_cs within the α′–α crystal formation transition range, more α′ form PLLAs were formed in PLLA/GNS-0.1 wt% than in pure PLLA. At T_cs higher but near the transition range, α′ form PLLA formation in the pure PLLA sample is too less to be detected, while in PLLA/GNS-0.1 wt% samples the α′ form PLLA content is increased due to the addition of GNSs. Thus, the α′–α crystal formation transition of PLLA in PLLA/GNS-0.1 wt% samples is shifted to a higher temperature than that of the pure PLLA sample.

With the kinetically formed α′ crystal and thermodynamically formed α crystal of PLLA in mind, it is of value to compare the effect of GNSs with the effects of PDLLA and DBS. It can be proposed that GNSs could promote formation of α′ crystal more than that of α crystal by enhancing the mobility of PLLA chain and thus accelerating α′ crystal crystallization more. PDLLA and DBS favor formation of α crystal because they can inhibit crystallization of α′ crystal more than that of α crystal. All GNSs, PDLLA and DBS play their roles by mainly affecting formation of α′ crystal. This is why GNSs in PLLA resulted in a shift of α′–α crystal formation transition towards high temperatures, and inversely in PDLLA or DBS. If one compares the effect of GNSs with that of melt shear on the crystal structure and crystallization rate of PLLA,[5,19] it can be concluded that both of them could accelerate nucleation of PLLA, but melt shear cannot accelerate spherulite growth[19] while GNSs can increase both the nucleation density and spherulite growth rate. This is because the influences of pre-ordered PLLA melt from melt shear are different from the influences of the increase of PLLA chain mobility on nucleation density and spherulite growth rate of PLLA, which also explain the shift of α′–α crystal formation transition towards high or low temperatures resulting from the existence of GNSs or melt shear in PLLA, respectively.

4. Conclusions

Graphene nanosheets (GNSs) are added into poly(L-lactide) (PLLA) by solution blending and a PLLA/GNS composite with GNS content of 0.1 wt% was obtained. The crystalline structures and crystallization behaviors of PLLA in PLLA/GNS composites were investigated and compared with those of pure PLLA. It was found that the formation of α′ form PLLA seems to be more preferred than that of α form PLLA in PLLA/GNSs at some T_cs due to the existence of GNSs, resulting in an observable shift of the α′–α crystal formation transition region of PLLA to high T_cs in PLLA/GNSs compared with that in pure PLLA. POM observations revealed that PLLA spherulites of α crystal were formed in PLLA/GNS composites as well as in pure PLLA and the added GNSs can obviously accelerate the crystallization process of α form PLLA in PLLA/GNSs, including both the nucleation density and the spherulite growth rate u increased due to the increase of the mobility of PLLA chains resulting from the existence of GNSs in PLLA and prior to steric hindrance of GNSs; but, GNSs seemed to have no observable influence on the zero growth temperature T_{zg} of PLLA which tends to be lower than the equilibrium melting point of PLLA. The SAXS results revealed that the long period L of PLLA in PLLA/GNS composites is much smaller than that in pure PLLA, which can be interpreted successfully by the Dual-lamellar stack model. Investigations on the melting behaviors of PLLA in both PLLA/GNSs and pure PLLA indicated that α′ form PLLA in PLLA/GNS composites isothermally crystallized at different T_cs within the temperature range of the α′–α crystal formation transition region which seem to be more perfect than the α′ crystals in pure PLLA, while the α form PLLA in PLLA/GNSs seems to be less perfect than the α crystals in pure PLLA. The general T_c dependent behaviors of formation of α′ form and α form PLLA in PLLA/GNSs were not changed and they were similar to those in pure PLLA.

Acknowledgements

This work was supported by the National Natural Science Foundation of China (51173130, 21274149, and 21374077).

References

1 P. Xiao, H. Li, S. Huang, H. Wen, D. Yu, Y. Shang, J. Li, Z. Wu, L. An and S. Jiang, *CrystEngComm*, 2013, **15**(39), 7914–7925.
2 H. Abe, Y. Kikkawa, Y. Inoue and Y. Doi, *Biomacromolecules*, 2001, **2**(3), 1007–1014.
3 W. Hoogsteen, A. Postema, A. Pennings, G. Tenbrinke and P. Zugenmaier, *Macromolecules*, 1990, **23**(2), 634–642.
4 P. Pan, B. Zhu, W. Kai, T. Dong and Y. Inoue, *Macromolecules*, 2008, **41**(12), 4296–4304.
5 S. Huang, H. Li, S. Jiang, X. Chen and L. An, *Polymer*, 2011, **52**(15), 3478–3487.
6 P. Pan, Z. Liang, B. Zhu, T. Dong and Y. Inoue, *Macromolecules*, 2009, **42**(9), 3374–3380.
7 J. Zhang, K. Tashiro, H. Tsuji and A. Domb, *Macromolecules*, 2007, **40**(4), 1049–1054.
8 W. Lai, *J. Phys. Chem. B*, 2011, **115**(38), 11029–11037.
9 I. Kim and Y. Jeong, *J. Polym. Sci., Part B: Polym. Phys.*, 2010, **48**(8), 850–858.
10 J. Xu, T. Chen, C. Yang, Z. Li, Y. Mao, B. Zeng and B. Hsiao, *Macromolecules*, 2010, **43**(11), 5000–5008.
11 T. Villmow, P. Pötschke, S. Pegel, L. Häussler and B. Kretzschmar, *Polymer*, 2008, **49**(16), 3500–3509.
12 T. Kawai, N. Rahman, G. Matsuba, K. Nishida, T. Kanaya, M. Nakano, H. Okamoto, J. Kawada, A. Usuki, N. Honma, K. Nakajima and M. Matsuda, *Macromolecules*, 2007, **40**(26), 9463–9469.
13 P. Pan, W. Kai, B. Zhu, T. Dong and Y. Inoue, *Macromolecules*, 2007, **40**(19), 6898–6905.
14 J. Zhang, K. Tashiro, H. Tsuji and A. Domb, *Macromolecules*, 2008, **41**(4), 1352–1357.
15 J. Zhang, Y. Duan, H. Sato, H. Tsuji, I. Noda, S. Yan, *et al.*, *Macromolecules*, 2005, **38**(19), 8012–8021.
16 J. Zhang, H. Tsuji, I. Noda and Y. Ozaki, *Macromolecules*, 2004, **37**(17), 6433–6439.
17 L. Cartier, T. Okihara, Y. Ikada, H. Tsuji, J. Puiggali and B. Lotz, *Polymer*, 2000, **41**(25), 8909–8919.
18 T. Cho and G. Strobl, *Polymer*, 2006, **47**, 1036–1043.
19 Y. Zhong, H. Fang, Y. Zhang, Z. Wang, J. Yang and Z. Wang, *ACS Sustainable Chem. Eng.*, 2013, **1**, 663–672.
20 M. Allen, V. Tung and R. Kaner, *Chem. Rev.*, 2010, **110**(1), 132–145.

21 H. Kim, A. Abdala and C. Macosko, *Macromolecules*, 2010, **43**(16), 6515–6530.
22 Z. Xu and C. Gao, *Macromolecules*, 2010, **43**(16), 6716–6723.
23 J. Xu, C. Chen, Y. Wang, H. Tang, Z. Li and B. Hsiao, *Macromolecules*, 2011, **44**(8), 2808–2818.
24 S. Stankovich, D. Dikin, G. Dommett, K. Kohlhaas, E. Zimney, E. Stach, R. Piner, S. Nguyen and R. Ruoff, *Nature*, 2006, **442**(7100), 282–286.
25 S. Kharchenko, J. Douglas, J. Obrzut, E. Grulke and K. Migler, *Nat. Mater.*, 2004, **3**(8), 564–568.
26 L. Li, B. Li, M. Hood and C. Li, *Polymer*, 2009, **50**(4), 953–965.
27 Y. Chen, G. Zhong, J. Lei, Z. Li and B. Hsiao, *Macromolecules*, 2011, **44**(20), 8080–8092.
28 L. Li, C. Li and C. Ni, *J. Am. Chem. Soc.*, 2006, **128**(5), 1692–1699.
29 N. Patil, L. Balzano, G. Portale and S. Rastogi, *Carbon*, 2010, **48**(14), 4116–4128.
30 M. C. Garcia-Gutierrez, J. J. Hernandez, A. Nogales, P. Pantine, D. R. Rueda and T. A. Ezquerra, *Macromolecules*, 2008, **41**(3), 844–851.
31 J. Hernandez, M. Garcia-Gutierrez, A. Nogales, D. Rueda and T. Ezquerra, *Macromolecules*, 2009, **42**(13), 4374–4376.
32 R. Haggenmueller, J. Fischer and K. Winey, *Macromolecules*, 2006, **39**(8), 2964–2971.
33 A. Karatrantos, R. J. Composto, K. I. Winey and N. Clarke, *Macromolecules*, 2011, **44**(24), 9830–9838.
34 D. Xu and Z. Wang, *Polymer*, 2008, **49**(1), 330–338.
35 A. Rozanski, B. Monasse, E. Szkudlarek, A. Pawlak, E. Piorkowska, A. Galeski, *et al.*, *Eur. Polym. J.*, 2009, **45**(1), 88–101.
36 N. Stribeck, A. Zeinolebadi, M. Sari, S. Botta, K. Jankova, S. Hvilsted, A. Drozdov, R. Klitkou, C. Potarniche, J. Christiansen and V. Ermini, *Macromolecules*, 2012, **45**(2), 962–973.
37 R. Nowacki, B. Monasse, E. Piorkowska, A. Galeski and J. Haudin, *Polymer*, 2004, **45**(14), 4877–4892.
38 J. Potts, S. Murali, Y. Zhu, X. Zhao and R. Ruoff, *Macromolecules*, 2011, **44**(16), 6488–6495.
39 H. Wang and Z. Qiu, *Thermochim. Acta*, 2011, **526**(1–2), 229–236.
40 H. Chen, W. Zhang, X. Du, J. Yang, N. Zhang, T. Huang and Y. Wang, *Thermochim. Acta*, 2013, **566**, 57–70.
41 A. Wurm, M. Ismail, B. Kretzschmar, D. Pospiech and C. Schick, Retarded, *Macromolecules*, 2010, **43**(3), 1480–1487.
42 P. Zhu, A. Phillips and G. Edward, *J. Chem. Phys.*, 2012, **136**(5), 054903.
43 M. D'Haese, P. Van Puyvelde and F. Langouche, *Macromolecules*, 2010, **43**(6), 2933–2941.
44 Y. Li, *Polymer*, 2011, **52**(10), 2310–1318.
45 P. Zhu, J. Tung, G. Edward and L. Nichols, *J. Appl. Phys.*, 2008, **103**(12), 124906–124914.
46 S. Nakagawa, K. Kadena, T. Ishizone, S. Nojima, T. Shimizu, K. Yamaguchi and S. Nakahama, *Macromolecules*, 2012, **45**(4), 1892–1900.
47 S. Nojima, Y. Ohguma, K. Kadena, T. Ishizone, Y. Iwasaki and K. Yamaguchi, *Macromolecules*, 2010, **43**(8), 3916–3923.
48 Y. Takenaka, H. Miyaji, A. Hoshino, A. Tracz, J. K. Jeszka and I. Kucinska, *Macromolecules*, 2004, **37**(26), 9667–9669.
49 J. Yang, S. Lin and Y. Lee, *J. Mater. Chem.*, 2012, **22**, 10805–10815.
50 H. Wang and Z. Qiu, *Thermochim. Acta*, 2012, **527**, 40–46.
51 T. Cho, W. Stille and G. Strobl, *Colloid Polym. Sci.*, 2007, **285**, 931–934.
52 G. Strobl and T. Y. Cho, *Eur. Phys. J. E*, 2007, **23**, 55–65.
53 H. Wen, S. Jiang, Y. Men, X. Zhang, L. An and Z. Wu, *J. Chem. Phys.*, 2009, **130**(16), 164909.
54 J. Kobayashi, T. Asahi, M. Ichiki, A. Okikawa, H. Suzuki, T. Watanabe, E. Fukuda and Y. Shikinami, *J. Appl. Phys.*, 1995, **77**, 2957–2973.
55 C. Marega, A. Marigo, V. Di Noto and R. Zannett, *Makromol. Chem.*, 1992, **193**, 1599–1606.
56 J. Zhang, K. Tashiro, A. Domb and H. Tsuji, *Macromol. Symp.*, 2006, **242**(1), 274–278.
57 Y. Ohtani, K. Okumura and K. Kawaguchi, *J. Macromol. Sci. Phys.*, 2003, **42**(3–4), 875–888.
58 D. Dikovsky, G. Marom, C. Avila-Orta, R. Somani and B. Hsiao, *Polymer*, 2005, **46**, 3096–3104.
59 A. Patti, *J. Phys. Chem. B*, 2014, **118**, 3731–3742.
60 H. Xiao, W. Lu and J. Yeh, *J. Appl. Polym. Sci.*, 2009, **113**, 112–121.
61 H. Tsuji and S. Miyauchi, *Polym. Degrad. Stab.*, 2001, **71**, 415–424.
62 B. Chu and B. Hsiao, *Chem. Rev.*, 2001, **101**(6), 1727–1762.

